Supplementary data

Divergent Pathogenic Dynamics of Immature Tick-Borne and Mosquito-Borne Flaviviruses: A Paradigm Shift in prM-Containing Particle Infectivity

Jiří Holoubek[1,2,3], Jiří Salát[1,2,3], Milos Matkovic[4], Petr Bednář[1,2,3], Pavel Novotný[5,6], Martin Hradilek[5], Taťána Majerová[5], Ebba Rosendal[7], Luděk Eyer[1,2,3], Andrea Fořtová[1,2,3], Michaela Dušková[1,2,3], Lesley Bell-Sakyi[8], Anna K. Överby[7], Andrea Cavalli[4,9] and Daniel Růžek[1,2,3]

[1]Department of Experimental Biology, Faculty of Science, Masaryk University, CZ-62500, Brno, Czech Republic

[2]Laboratory of Emerging Viral Diseases, Veterinary Research Institute, CZ-62100, Brno, Czech Republic

[3]Institute of Parasitology, Biology Centre of the Czech Academy of Sciences, CZ-37005, Ceske Budejovice, Czech Republic

[4]Institute for Research in Biomedicine, Università della Svizzera Italiana, Bellinzona, Switzerland

[5]Institute of Organic Chemistry and Biochemistry of the Czech Academy of Sciences, CZ-16610, Prague, Czech Republic

[6]Department of Physical and Macromolecular Chemistry, Faculty of Science, Charles University, CZ-12843, Prague, Czech Republic

[7]Department of Clinical Microbiology, Laboratory for Molecular Infection Medicine Sweden (MIMS), Umeå University, SE-90187, Umeå, Sweden

[8]Department of Infection Biology and Microbiomes, Institute of Infection, Ecological and Veterinary Sciences, University of Liverpool, Liverpool L3 5RF, United Kingdom

[9]Swiss Institute of Bioinformatics, Lausanne, Switzerland

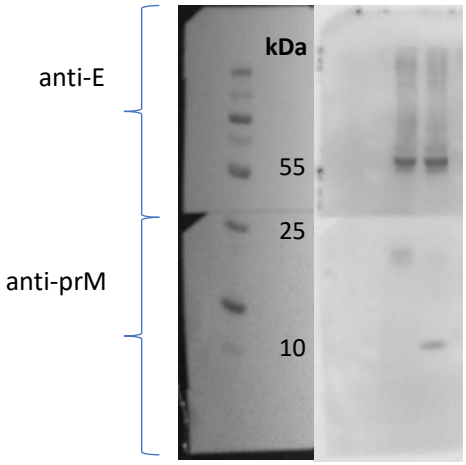

Supplementary Fig. 1 | Unmodified western blot image corresponding to Fig. 1b. Western blot membrane was divided into two parts to enable separate incubation with different primary and secondary antibodies. Image was acquired with a GE Amersham imager 680.

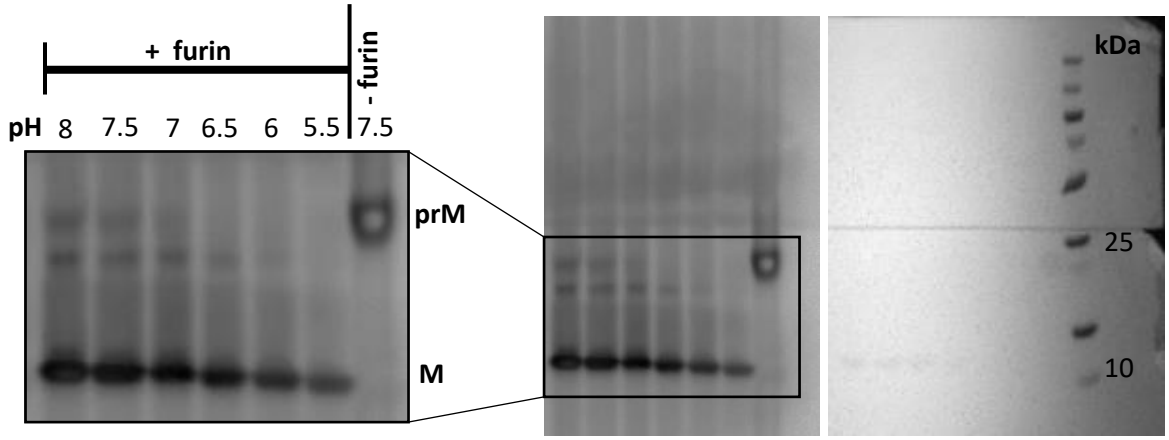

Supplementary Fig. 2 | pH dependence of furin cleavage of prM-TBEV. Western blot analysis showed efficient furin cleavage over the entire pH range from 5.5 to 8.

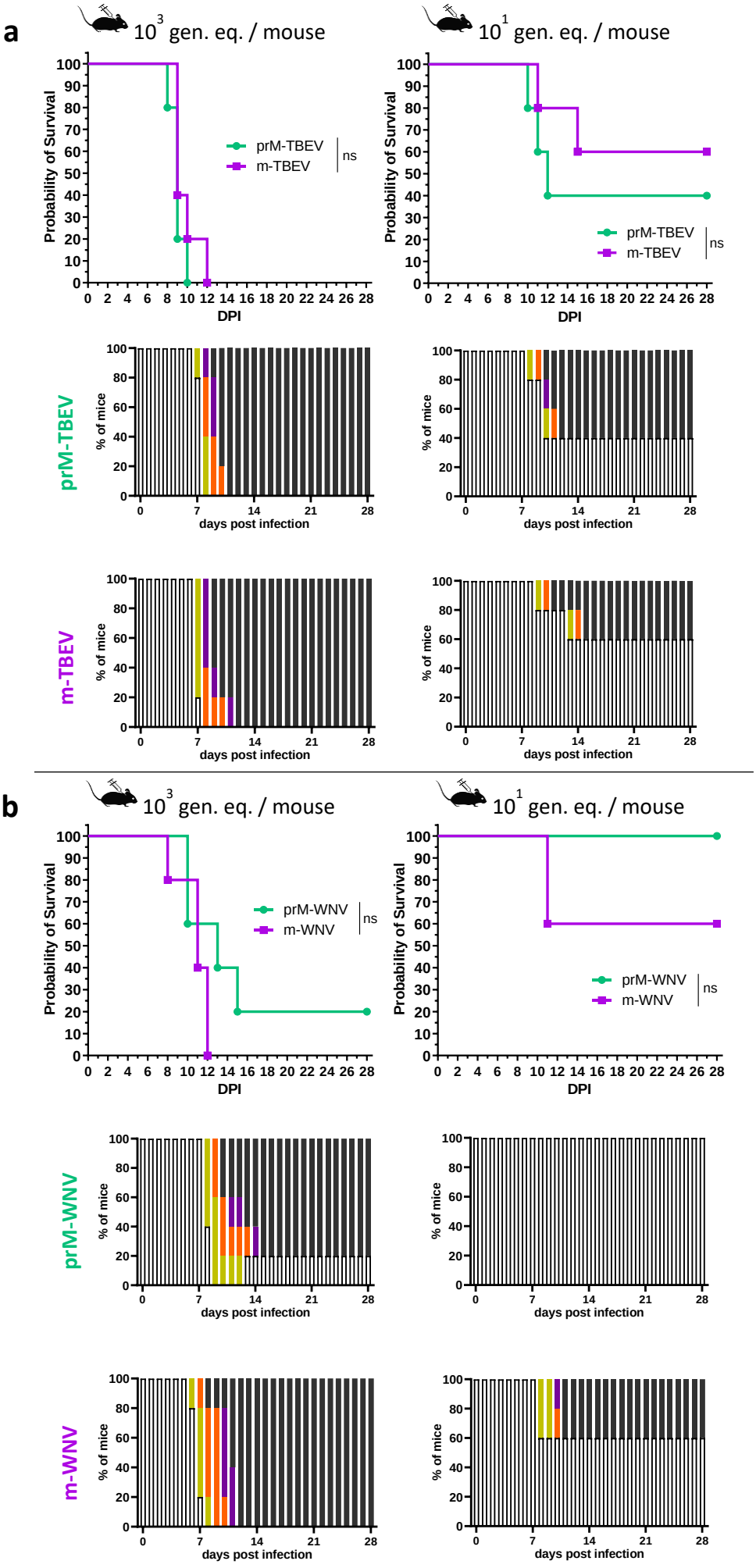
a
10^3 gen. eq. / mouse
10^1 gen. eq. / mouse
Probability of Survival
DPI
prM-TBEV
m-TBEV
ns
% of mice
days post infection
b
prM-WNV
m-WNV

Supplementary Fig. 3 | Comparison of the pathogenicity of prM-TBEV/m-TBEV and prM-WNV/m-WNV in a mouse model. **a,** Four groups of adult BALB/c mice (n = 5, 5) were subcutaneously infected with two different doses (10^1 and 10^3 genome equivalents per mouse) of prM-TBEV (two groups) or m-TBEV (two groups), respectively. In the case of prM-TBEV, the infectious dose calculation corresponds to ~ 4 and 400 PFU for 10^1 and 10^3 gen. eq. per mouse, respectively. Survival rates and clinical scores were monitored for 28 days. Clinical score was evaluated as follows: 1, no signs; 2, piloerection; 3, hunched back; 4, paralysis; and 5, death **b,** Similar to the above experiment, four groups of mice were infected with either prM-WNV or m-WNV, and survival was monitored for 28 days. In the case of prM-WNV, the infectious dose calculation corresponds to ~ 0.07 and 7 PFU for 10^1 and 10^3 gen. eq. per mouse, respectively. Clinical signs of disease were assessed as described above. Survival rates were statistically evaluated using the log-rank Mantel-Cox test.

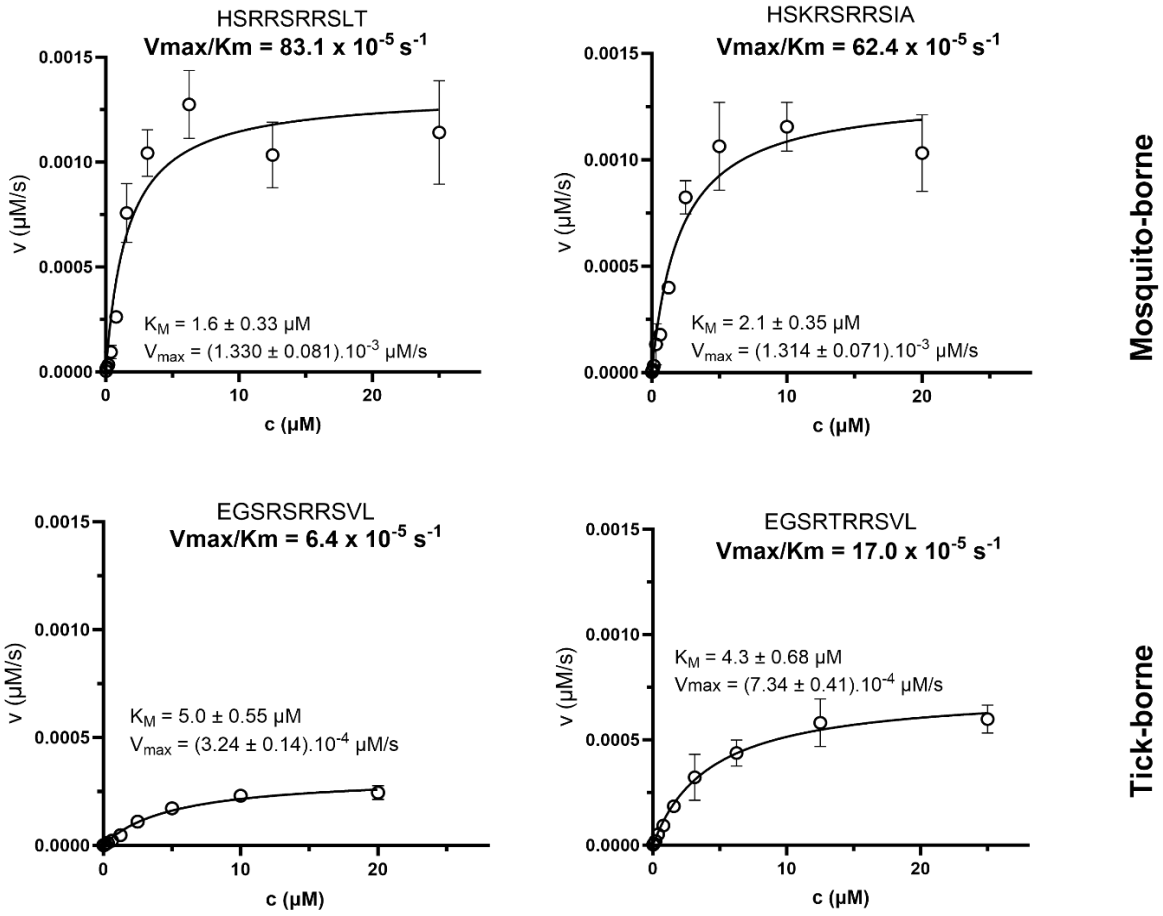

Supplementary Fig. 4 | Determination of Km/Vmax values. The substrate-dose-dependent initial velocity of cleavage was measured at pH 7.0 in buffer (25 mM acetic acid, 25 mM MES, 25 mM glycine, 1 mM $CaCl_2$) for each peptide substrate, in triplicate. Reactions were started by addition of furin (final concentration of 10 ng mL^{-1}). Km and Vmax values were fitted to the Michaelis-Menten equation using GraphpadPrism software. The resultant Vmax/Km indicates that the studied mosquito-borne prM-derived peptides were more efficiently cleaved by furin, compared to substrates derived from tick-borne flaviviruses.

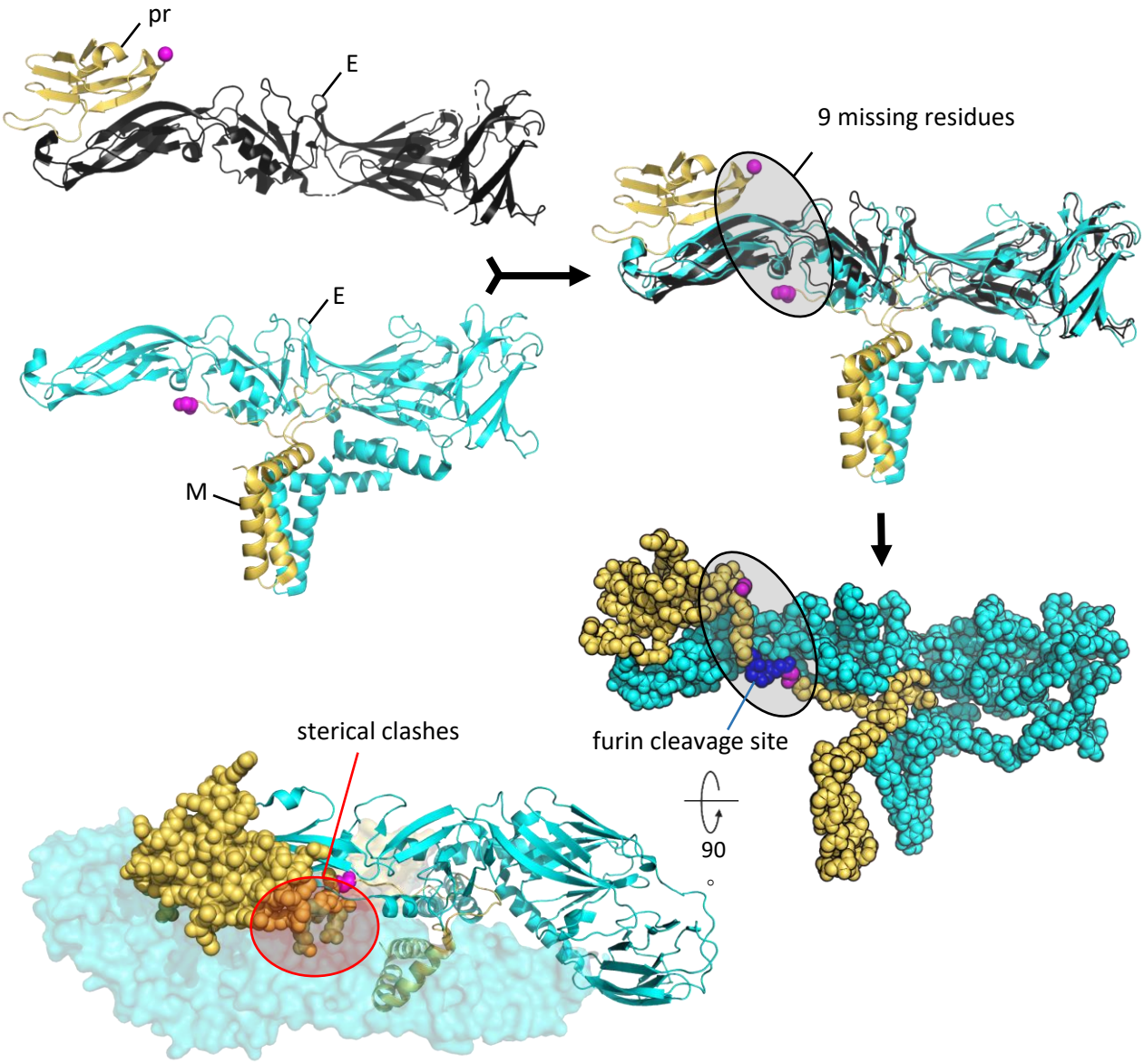

Supplementary Fig. 5 | Modelling the prM-E complex of the smooth immature particle. Currently, there is no experimental structure of the immature smooth flavivirus. Therefore, we used the E-pr structure available in PDB 7QRF, which is superimposed with the 7Z51 structure of the E-M complex. Nine residues are missing between the two magenta-coloured residues of these PDB structures. Using AlphaFold, we modelled the heterodimer prM-E and created a complete heterodimeric model together with the two PDB structures. The missing 9 residues do not have much conformational space for modelling because the distance between the purple residues is just enough to connect the 9 residues together. These nine residues are in the middle of the complete prM-E complex. Therefore, they would form clashes with the E protein in a smooth conformation unless they have been previously cleaved.

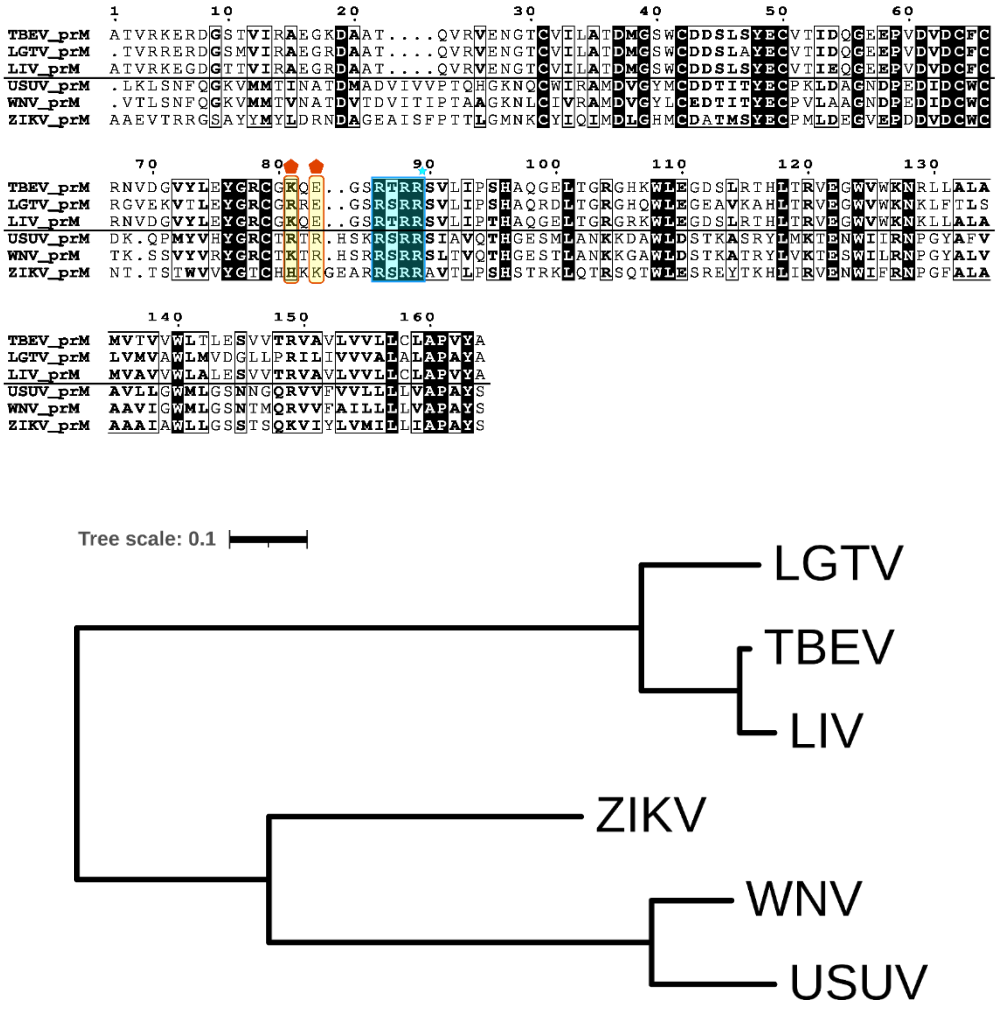

Supplementary Fig. 6 | Multiple sequence alignment of flavivirus prM proteins, with the highlighted furin cleavage site (blue) and amino acid residues K81 and E83 (orange), which were mutated in rTBEV. Percentage of equivalent residues was calculated considering the physico-chemical properties. Fully conserved residues are shown on a black background, and residues in black frames indicate that over 70% of residues share similar properties. Alignment was performed using ClustalW, with subsequent graphical rendering using ESPript 3.0. The numbering reflects the position within the alignment. The highlighted residues were numbered and used in the study based on the position of the respective residue in the amino acid sequence for a particular virus. The phylogenetic tree was based on amino acid multiple sequence alignment (prM protein) using MAFFT, and then constructed using the neighbor-joining method with JTT substitution model. Visualization and graphic processing were performed with the iTOL online tool[68].

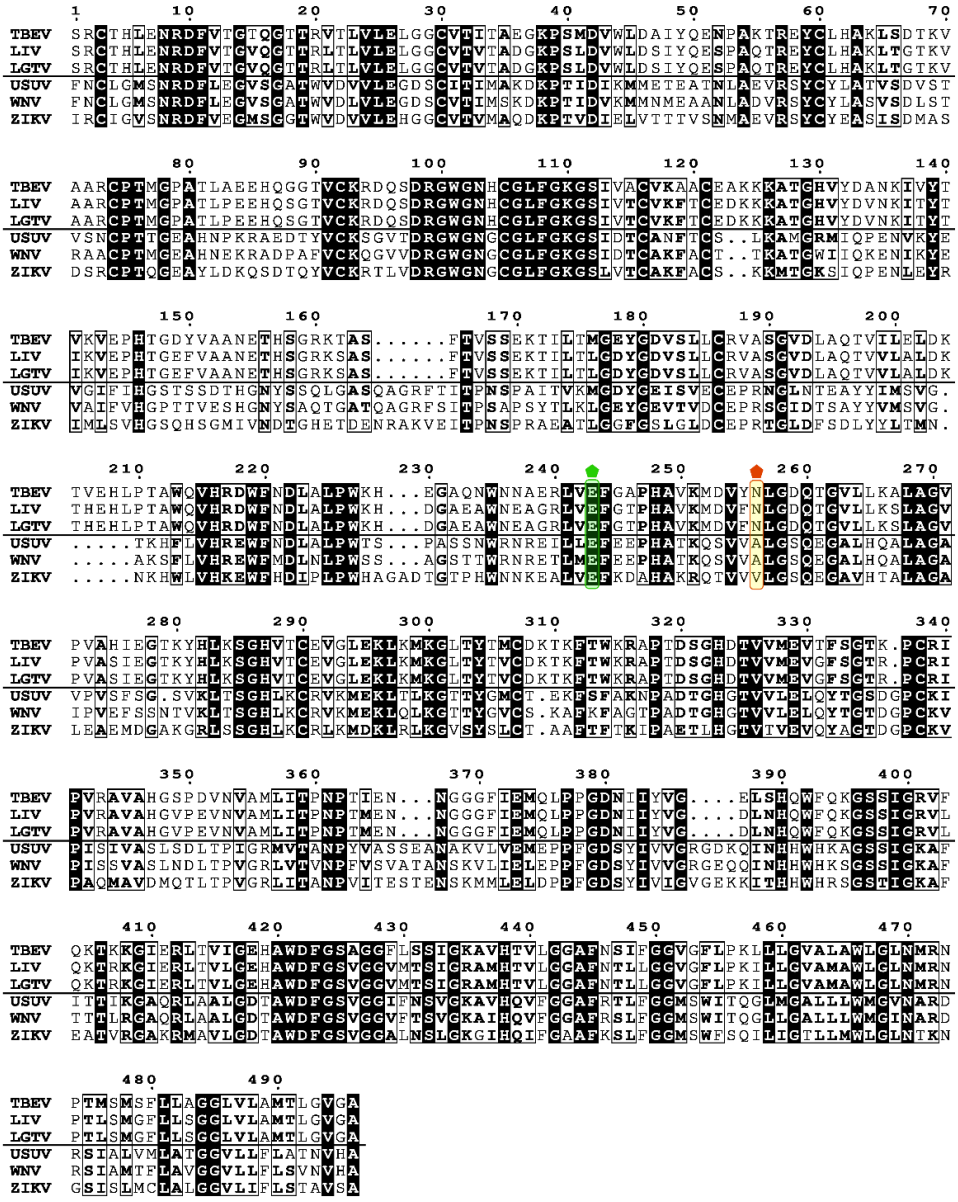
TBEV
LIV
LGTV
USUV
WNV
ZIKV

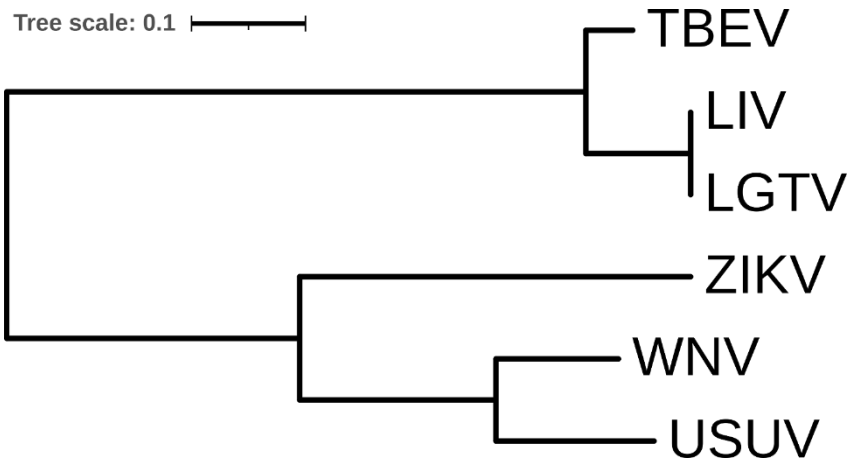
Tree scale: 0.1
TBEV
LIV
LGTV
ZIKV
WNV
USUV

Supplementary Fig. 7 | Multiple sequence alignment of flavivirus E proteins with highlighted TBEV residue E243, USUV residue E241 (green), and TBEV position N256 (orange) mutated in rTBEV. The percentage of equivalent residues was calculated considering the physicochemical properties. Fully conserved residues are shown on a black background, and residues in black frames indicate that over 70% of the residues have similar properties. The alignment was created using Clustal Omega, and then graphically processed with ESPript 3.0. The numbering reflects the position within the alignment. The highlighted residues were numbered and used in the study based on the position of the respective residue in the amino acid sequence for a particular virus. The phylogenetic tree was based on amino acid multiple sequence alignment (E protein) using MAFFT, and then constructed using the neighbor-joining method with JTT substitution model. Visualization and graphic processing were performed with the iTOL online tool.

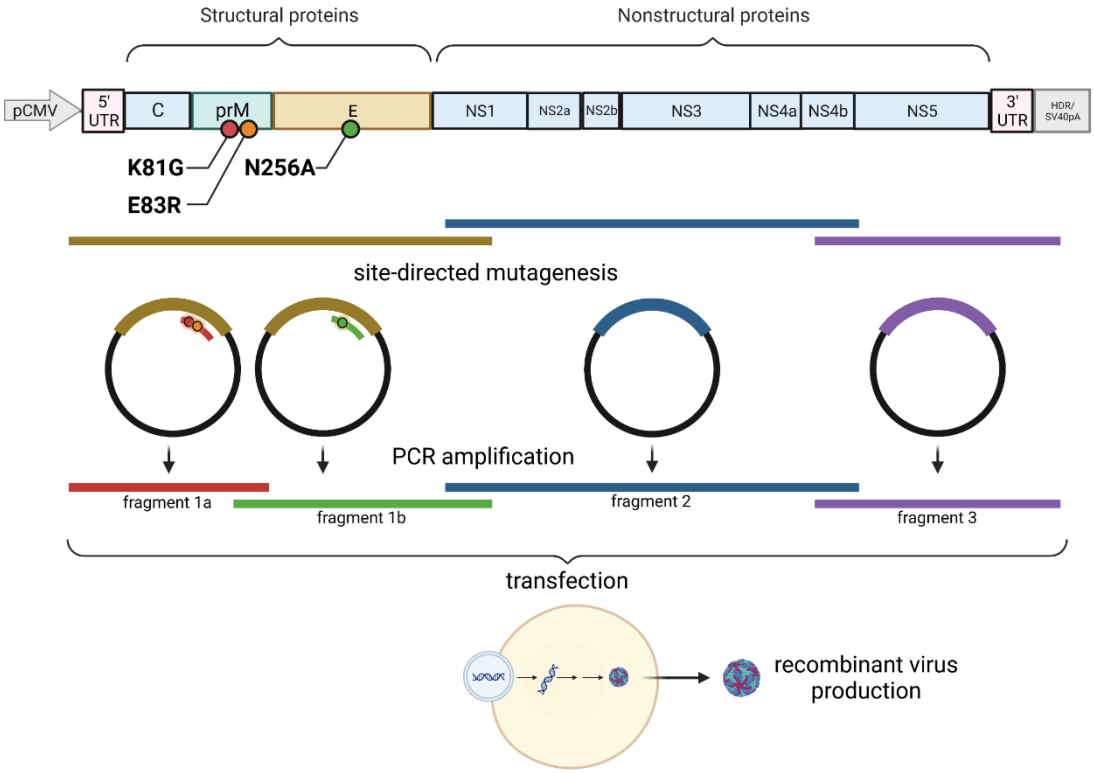

Supplementary Fig. 8 | Scheme representing the site-directed mutagenesis approach using infectious subgenomic amplicons. Mutated sites in the prM (K81G, E83R) and E (N256A) proteins were introduced using modified primers, and are highlighted. Overall, four amplified DNA fragments with overlapping ends were transfected into BHK-21 cells, followed by harvesting of the recombinant virus.

Supplementary Table 1 | Primers used to generate overlapping amplicons of TBEV fragments to produce recombinant virus rTBEV.

Primer ID	Sequence (5’ - 3’)
mut_prM_site_1+2_FWa	GGGGGTCAGCGTGGCTCACGGACAAGGCGC
mut_prM_site_1+2FWb	GGGGGTCAGCGTGGCTCACGGACAAGG
mut_prM_site_1+2_R	GCCACGCTGACCCCCACAGCGTCCATACTCC
mut_Env_site_3_FW	TGTACGCACTCGGAGACCAGACTGG
mut_Env_site_3_R	TCTCCGAGTGCGTACACATCCATC